Breakup of asymmetric liquid ligaments

Carole Planchette [1,*] Francesco Marangon [2] Wen-Kai Hsiao,[2] and Günter Brenn [1]
[1] *Institute of Fluid Mechanics and Heat Transfer, Graz University of Technology, Inffeldgasse 25/F, 8010 Graz, Austria*
[2] *Research Center for Pharmaceutical Engineering, Inffeldgasse 13, 8010 Graz, Austria*

(Received 1 August 2019; revised manuscript received 23 September 2019; published 19 December 2019)

The evolution of a finite liquid ligament into either a single drop or several droplets is driven by the competition of two simultaneous processes: the recoil and the pinch-off. Scalings providing the kinetics of each process can be compared to predict the breakup of cylindrical symmetric ligaments. Here, asymmetric ligaments formed by a main drop connected to a cylindrical tail and commonly produced by inkjet printing are considered. Using two print heads, 16 inks, and various printing parameters, we show the limits of commonly admitted scalings for asymmetric ligaments. The recoil is governed by a modified Taylor-Culick velocity and a complex drainage, possibly leading to pinch-off, develops at the junction of the ligament with the main drop. The ligament aspect ratio affects this process for which two regimes must be accounted for. Finally, the ratio between the recoil and pinch-off timescales successfully predicts asymmetric ligament breakup.

DOI: 10.1103/PhysRevFluids.4.124004

I. INTRODUCTION

In contrast to perfectly symmetric liquid ligaments which can only form under uniform environments, asymmetric ligaments are commonly encountered in nature and industrial processes [1,2]. The asymmetry arises as soon as a jet breaks up irregularly or as a drop is asymmetrically distorted. In this case, the competition between surface tension, which tends to limit distortion, and an opposing contribution gives rise to a simple morphology corresponding to a main drop connected to a cylindrical tail. The forces at stake can be as various as viscous shear [3], centrifugal force [4], gravity [5], aerodynamic drag [6], electrohydrodynamic force [7], or other dynamic effects found, for example, during drop impact [8]. The best-known process producing asymmetric ligaments and originally motivating this study is drop-on-demand inkjet printing [9]. Independently from the formation process, the ligament may recoil in the main drop or pinch-off into satellite droplets. In recent decades, this problem has become increasingly important due to the continuous development and emergence of three-dimensional (3D) printing. Its apparent versatility and flexibility makes inkjet printing an additive manufacturing method of choice for producing printed electronics, biochip arrays, printed medicines, and many others [10–13].

Experimental and numerical studies have demonstrated the influence of dynamic viscosity and surface tension on the liquid jettability [14–17]. Operability diagrams based on the Ohnesorge (Oh) and Weber (We) numbers provide a strong theoretical understanding of Newtonian inkjetting [18], but do not predict the subsequent evolution of the ejected liquid entity. Experimental and numerical studies report the performances of inkjet devices, but without addressing the formation of satellite droplets in the form of a general criterion [19,20]. Yet, satellite droplets originating from ligament

*carole.planchette@tugraz.at

breakup are critical to most applications, causing off-target deposition and volume deviation. Most studies, largely inspired by the knowledge of jet stability [21], focus on the breakup of finite, but symmetric liquid ligaments [2,19,22–26]. Beyond the lack of consensus for the parameter range of interest ($0.01 < \mathrm{Oh} < 0.5; 5 < \mathrm{We} < 50$), the applicability of these models remains limited since the ligaments produced at the print head are not symmetric. An extension to nonsymmetric cases was proposed by Hoath *et al.* [27], who considered the main drop as a plane of symmetry and compared the kinetics of recoil and pinch-off using a virtual ligament twice as long as the real one. This approach leads to a stability criterion which could not prove its efficacy while tested against our data. As a result, adjusting a given printer (voltage, duration, and shape of the pulse) to obtain satellite-free printing of a given ink still mainly relies on the empirical know-how of trained operators.

In this work, we address the critical issue of satellite droplet formation by studying in detail the dynamics of finite and asymmetric ligaments formed during inkjet printing. We show that the recoil timescale proposed by Hoath *et al.* [27] must be modified to account for finite-size and viscous effects. In contrast to existing models, we evidence that two regimes of pinch-off exist, and that the possible reopening of the neck separating the main drop from the ligament may stabilize the liquid system [28]. Scaling laws are proposed, resulting in a stability criterion which agrees very well with our data.

II. RESULTS AND DISCUSSION

The experimental results are obtained using two print heads from Microdrop Technologies GmbH, operated with voltage, duration, and frequency of electric pulses ranging from 80 to 110 V, 20 to 40 μs, and 100 to 1000 Hz, respectively. The drop formation is imaged using a standard camera and stroboscopic illumination. The tested inks correspond to 16 different solutions produced with various proportions of ultrapure water (from TKA purification unit), ethanol (analytical grade, Merck GmbH), and sugar (Wiener Zucker, Agrana AG). The density ρ, surface tension σ, and viscosity μ were measured enabling the calculation of the nozzle Ohnesorge number, $\mathrm{Oh}_n = \mu/\sqrt{\rho\sigma d_n}$, based on the inner nozzle diameter $d_n = 100\ \mu$m. The results are obtained for eight inks covering the maximal jettable range $0.074 \leqslant \mathrm{Oh}_n \leqslant 0.261$, identified by a broader screening ($0.04 \leqslant \mathrm{Oh}_n \leqslant 0.699$).

Once the ink is ejected from the nozzle, two typical behaviors can be observed. Either the ligament recoils into the main drop (duration τ_{recoil}) or it pinches off, giving rise to at least one satellite droplet (duration τ_{p-o}); see Fig. 1. Taking the instant when the ligament detaches from the nozzle as the reference time, the initial aspect ratio of the ligament is given by $\lambda = 2l_0/d$, with the length l_0 and the diameter d. Note that a possible recombination of the primary drop with the satellite(s) [29] is not considered in our study.

With the temporal evolution of the ligament length being linear [Fig. 2(a)], the experimental recoil velocity $V_{\mathrm{recoil}}^{\mathrm{expt}}$ can be uniquely measured for each case. The values are plotted against theoretical velocities. The Taylor-Culick velocity, $V_{\mathrm{Taylor}} = \sqrt{\sigma/\rho d}$, considered in [27,30], shows poor agreement with our data [Fig. 2(b)] and calls for an improved model as already evidenced in [28]. Deviations may be caused by the finite length of the ligament and by viscous effects, as already observed for recoiling liquid curtains [31]. To account for these effects, we propose to balance the unsteady term $\rho\partial u/\partial t \propto \rho V_{\mathrm{recoil}}^{\mathrm{theo}}/\sqrt{\rho d^3/\sigma}$ with the sum of the pressure gradient evaluated over the ligament length, $\partial p/\partial z \propto \sigma/dl_0$, and the viscous losses taken as $\mu\Delta V_{\mathrm{recoil}}^{\mathrm{theo}} \propto \mu V_{\mathrm{recoil}}/d^2$. We obtain, after linearization,

$$V_{\mathrm{recoil}}^{\mathrm{theo}} = \beta\sqrt{\sigma/\lambda\rho l_0}\,(1 + \alpha\mathrm{Oh}) + \gamma, \tag{1}$$

where $\mathrm{Oh} = \mu/\sqrt{\rho\sigma d}$ is the ligament Ohnesorge number calculated on its diameter d; $\alpha = 3.32$, $\beta = 4.59$, and $\gamma = 0.68\ \mathrm{m\ s^{-1}}$ are constants giving a quantitative agreement [Fig. 2(c)]. Note that if α and β are needed to evaluate the relative importance of the viscous and capillary contributions, γ represents (for drops of similar weight) the momentum transferred from the device to the drop

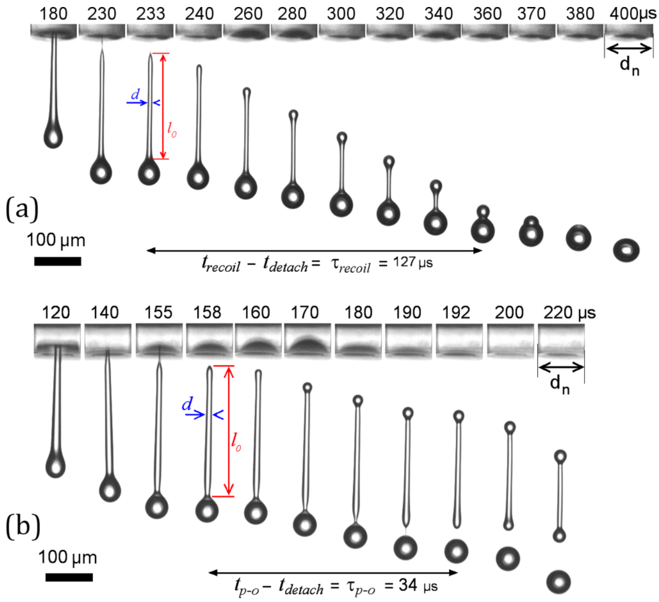

FIG. 1. Drop formation pictures showing (a) ligament recoil for $\mathrm{Oh}_n = 0.261$, with printer parameters 99 V, 33 μs, and 100 Hz; and (b) ligament pinch-off for $\mathrm{Oh}_n = 0.084$, with printer parameters 105 V, 36 μs, and 100 Hz. The initial dimensions of the ligament (l_0 and d) are indicated in both cases.

motion. In our study, γ is independent of the used print head and printing parameters, which might nevertheless not always be the case. Assuming the recoil is completed when the ligament has contracted over $l_0 - 2d$ provides, after simplification, the theoretical recoil timescale

$$\tau_{\mathrm{recoil}}^{\mathrm{theo}} = \beta^* \lambda l_0 \sqrt{\rho d/\sigma}(1 - \alpha^* \mathrm{Oh}) + \gamma^*, \tag{2}$$

where $\alpha^* = 0.65$, $\beta^* = 0.029$, and $\gamma^* = 25\times10^{-6}$ s are adjusted constants which must be empirically determined. Indeed, neglecting γ, approximating $l_0 - 2d$ by l_0 $(2d/l_0 < 0.2)$, and proceeding to the first-order linearization of Eq. (1) is too crude for deducing α^*, β^*, and γ^* from α, β, and γ. Yet, following this empirical step, the agreement with the experimental data is excellent; see Fig. 2(d).

In order to predict whether or not satellite droplets are formed, the recoil timescale must be compared to the one of pinch-off. The viscous scaling $\tau_{p-o}^{\mathrm{visc}} = \mu d/\sigma$, used in several studies [21,27], shows poor agreement with our data [see Fig. 3(a), inset]. The finite size or aspect ratio of the ligament is not considered by this scaling, while it is expected to play a role, at least via its simultaneous recoil in the main drop. To evaluate the role of the ligament length, $\tau_{p-o}^{\mathrm{expt}}$ is plotted against λ in Fig. 3(a). In contrast to the commonly admitted viscous pinch-off scaling, the measured timescale is found to strongly vary for a given liquid with λ, the ligament aspect ratio. Furthermore, the variations are not monotonic, but show a local maximum separating two regimes. Note that since the variations of the ligament diameter are very moderate ($d = \bar{d} \pm 25\%$, e.g., $10.5 < d < 13.5$ μm), λ measures the variations of the ligament length. We explain this observation by the influence of the recoiling flux on the viscocapillary squeezing of the neck. This flux can be associated to the kinetic pressure $\rho {V_{\mathrm{recoil}}}^2$, which may (or not) be sufficient to overcome the capillary overpressure building up at the neck and scaling at first order as σ/d. Using Eq. (1) and neglecting γ, the transition is found for

$$\lambda^* = A(1 + \alpha \mathrm{Oh}). \tag{3}$$

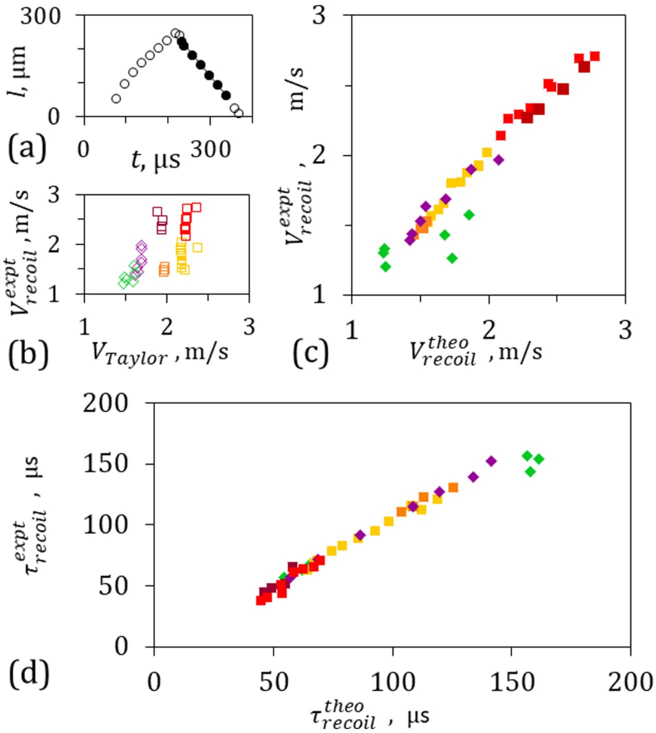

FIG. 2. (a) Temporal evolution of the ligament length obtained from the pictures of Fig. 1(a) showing a constant recoil velocity (full points and fit). (b) $V_{\text{recoil}}^{\text{expt}}$ as a function of V_{Taylor}. (c) $V_{\text{recoil}}^{\text{expt}}$ as a function of $V_{\text{recoil}}^{\text{theo}}$ [Eq. (1)]. (d) $\tau_{\text{recoil}}^{\text{expt}}$ as a function of $\tau_{\text{recoil}}^{\text{theo}}$ [Eq. (2)]. Squares correspond to device 1 and diamonds to device 2. Oh_n is varied as follows: 0.124 (green), 0.148 (yellow), 0.155 (orange), 0.216 (red), 0.232 (purple), and 0.261 (brown).

Taking $A = 18.5$ and keeping $\alpha = 3.32$ as in Eq. (1), we obtain, for each liquid, the transition represented by the vertical line of the same color; see Fig. 3(a). Despite the extreme simplicity of this approach and its inherent approximations, the agreement is good and validates the hypothesis that the ligament recoil influences its pinch-off. As a consequence, two regimes must be considered. For $\lambda < A(1 + \alpha\text{Oh})$, referred to as "short ligaments," the kinetic pressure is strong enough to let the recoiling flux directly enter the main drop. The pinch-off timescale can thus be deduced by balancing the capillary pressure gradient σ/dl_0 with the viscous losses $\mu d\lambda/\sigma$ evaluated with the axial velocity component u. The resulting modified viscocapillary timescale is $\mu d\lambda/\sigma$, which can be approximated by

$$\tau_{p-o}^{\text{short}} = \frac{\mu \bar{d}\lambda}{\sigma}, \tag{4}$$

where d is replaced by $\bar{d}$, the average ligament diameter, to limit the experimental uncertainty on d. The results are plotted in Fig. 3(b), using $\bar{d} = 12.6\ \mu$m and no adjustable factor or constant. The agreement is excellent for the encircled points, which correspond to short ligaments. The inset pictures evidence the cylindrical shape of the ligament and support the assumption of a direct drainage into the main drop.

For cases where $\lambda > A(1 + \alpha\text{Oh})$, also called "long ligaments," the capillary pressure at the neck is large enough to prevent the recoiling flux from entering the main drop. Instead, the flux accumulates in front of the neck, creating a visible bulge, as displayed in the inset of Fig. 3(c). Integrated over t, the process time, it produces a volume $\Omega_{\text{recoil}}(t) = \pi d^2 V_{\text{recoil}} t/4$, which

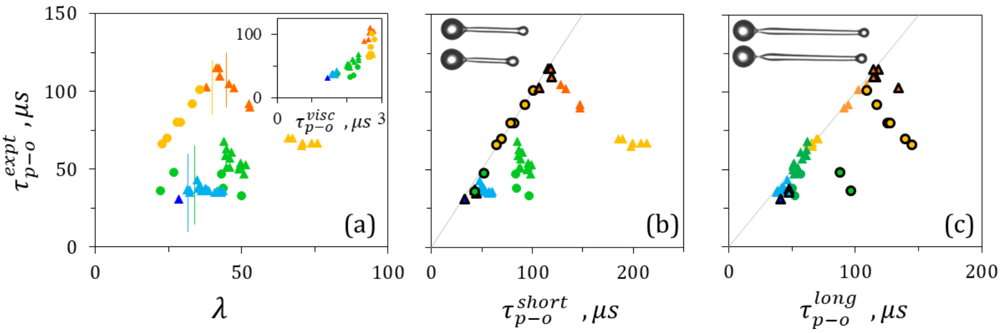

FIG. 3. (a) τ_{p-o}^{expt} as a function of λ for different liquids and devices. The vertical lines correspond to Eq. (3) evaluated with $A = 18.5$, $\alpha = 3.32$ and Oh corresponding to each liquid. Inset: τ_{p-o}^{expt} as a function of τ_{p-o}^{visc}. (b) τ_{p-o}^{expt} as a function of $\tau_{p-o}^{\text{short}}$ [Eq. (4)]. (c) τ_{p-o}^{expt} as a function of τ_{p-o}^{long} [Eq. (6), with $\tilde{\beta} = 1.63\times10^{-4}$ and $\tilde{\gamma} = 5\times10^{-6}$ s]. For all graphs, Oh_n varies as follows: 0.074 (dark blue), 0.084 (light blue), 0.097 (green), 0.124 (yellow), and 0.219 (orange). Triangles indicate data from device 1, circles from device 2. For (b) and (c), the points encircled (not encircled) by a black line correspond to short (long) ligaments.

corresponds to the accumulated volume $\Omega_{\text{visc}}(t) = \pi d^{*2} l_{\text{visc}}(t)/4$. Here, d^* is the locally enlarged ligament diameter and $l_{\text{visc}}(t) = \sqrt{\mu t/\rho}$ is the thickness of the viscous boundary layer developing in front of the neck. Using Eq. (1) with, for simplicity, $\gamma = 0$ and $\alpha\text{Oh} > 1$ (viscous regime), yields

$$\left(\frac{d^*}{d}\right)^2 = \alpha\text{Oh}\sqrt{\frac{\sigma\, t}{\mu\lambda l_0}}. \tag{5}$$

Note that beside these simplifications, the linear relation between the theoretical and experimental recoiling velocity is satisfyingly preserved. Further, replacing d by $d^*(\tau_{p-o}^{\text{long}})$ in τ_{p-o}^{visc}, the classical viscous timescale provides the long ligament pinch-off timescale,

$$\tau_{p-o}^{\text{long}} = \tilde{\beta}\frac{\mu d}{\sigma}\left(\frac{\text{Oh}}{\lambda}\right)^{2/3} + \tilde{\gamma}. \tag{6}$$

The scaling of Eq. (6) is tested in Fig. 3(c), where τ_{p-o}^{expt} is plotted against τ_{p-o}^{long}, using $\tilde{\beta} = 890$ and $\tilde{\gamma} = 5\times10^{-6}$ s. The agreement is very good for all of the not encircled points, which correspond to long ligaments.

Having understood and modeled the ligament recoil and pinch-off, a criterion for satellite droplet formation is established. It relies on the relative kinetics of the two competing processes and consists of the ratio $\tau_{p-o}^{\text{theo}}/\tau_{\text{recoil}}^{\text{theo}}$, where $\tau_{\text{recoil}}^{\text{theo}}$ is evaluated according to Eq. (2) with $\gamma^* = 0$ for simplicity, and τ_{p-o}^{theo} is taken as τ_{p-o}^{long} [Eq. (6) with $\tilde{\gamma} = 0$ for simplicity] or $\tau_{p-o}^{\text{short}}$ [Eq. (4)], when the ligament is defined as long or short, respectively. The criterion is tested against all our experimental data in Fig. 4(a). For $\tau_{p-o}^{\text{theo}}/\tau_{\text{recoil}}^{\text{theo}} < 1$, the ligament does not have time to recoil, and breakup is predicted in excellent agreement with the data. Below the line representing $\tau_{\text{recoil}}^{\text{theo}}/\tau_{p-o}^{\text{theo}} = 1$, satellite droplets are formed (full symbols), and so for both short (gray) and long (black) ligaments. On the contrary, for $\tau_{p-o}^{\text{theo}}/\tau_{\text{recoil}}^{\text{theo}} > 1$, the ligament always completes its recoil and no satellite droplets are formed (empty symbols).

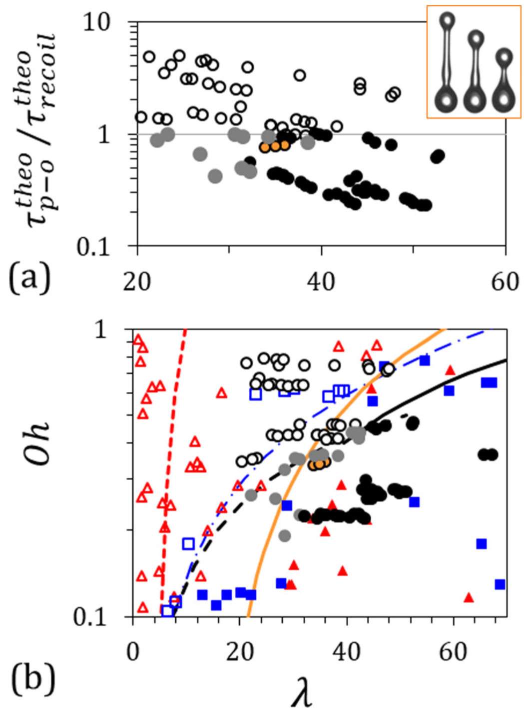

FIG. 4. (a) Our data in the form of $\tau_{p-o}^{\rm theo}/\tau_{\rm recoil}^{\rm theo}$ as a function of λ. Inset: Images evidencing the neck reopening, taken at $t = 97$, 117, and 137 μs for $\mathrm{Oh}_n = 0.124$, 88 V, 25 μs, 100 Hz with device 2. (b) Same data plotted as a (Oh;λ) map. Additional data from asymmetric (blue) [27] and symmetric (red) [2] ligaments. The red dashed line corresponds to the linear stability theory [19], the orange continuous line to the one of [28], the gray one to the criterion of [27], and the dashed (continuous) black lines to our criterion for short (long) ligaments (gray and black symbols). Full symbols correspond to pinch-off, empty ones to recoil; circles filled with orange correspond to observed neck reopening.

We plot in Fig. 4(b) our data as a (Oh, λ) map to include existing data from the literature obtained on symmetric [2] and asymmetric [27] ligaments. For further comparison, the linear stability analysis of symmetric ligaments [19] (red dashed line) and the criterion of Hoath *et al.* based on the comparison of the simple recoil and pinch-off kinetics [27] (blue dot-dashed line) are tested. Neglecting γ^* and $\tilde{\gamma}$, our model can be rewritten as $\lambda_c = 2/[\beta(1/\mathrm{Oh} - \alpha^*)]$ (dashed black line) for short ligaments and approximated by $\lambda_c = \{2\tilde{\beta}/[\beta^*(1 - \alpha^*\mathrm{Oh})]\}^{3/8}\mathrm{Oh}^{5/8}$ (continuous black line) for long ones. The absence and formation of satellites cannot be distinguished by the linear stability analysis and are only partly separated by the criterion from Hoath *et al.* Indeed, for $0.2 < \mathrm{Oh} < 0.4$, the most relevant domain for inkjet printing, it fails in predicting satellite formation. In contrast, our criterion works very well, except for a few points which can easily be explained. For long ligaments, a few points from Hoath *et al.* show breakup, while recoil is predicted. Besides large experimental uncertainty on d [27] and the approximations made by neglecting $\tilde{\gamma}$ and γ^*, which should, in fact, be compared to $\tau_{\rm sigma} = \sqrt{\rho d^3/\sigma}$, the pinch-off may take place away from the junction with the main drop, making our approach irrelevant [19,28] and explaining why symmetric ligaments are also found to recoil in this domain. Finally, three points, indicated by black crosses on top of yellow squares and corresponding to recoil, are predicted as pinch-off. This discrepancy is caused by the reopening of the neck, as described in [28] and illustrated in the inset of Fig. 4(a). The bulge forming just before the neck migrates toward the main drop and reopens the neck. This phenomenon, attributed to a Venturi effect [28], sufficiently delays the ligament pinch-off to enable its total recoil. No analytical model exists to predict its occurrence and, in our experiments, these points are found for $\lambda \approx \lambda^*$, i.e., close to the transition between bulge formation and direct recoil.

III. CONCLUSIONS

In conclusion, we have shown that the kinetics of recoil and pinch-off of asymmetric ligaments are not well estimated by the scalings commonly used for symmetric ligaments. We proposed modification to account for viscous and finite-size effects, and, more importantly, for the presence of the main drop at one ligament extremity. The effects of the asymmetric ligament recoil on its pinch-off have been unraveled, evidencing the existence of two regimes, universally separated by a critical ligament aspect ratio. Further, a simple, yet efficient criterion for the breakup of asymmetric ligaments has been established, which is of great practical interest for inkjet printing. Enabling a quick, reliable, and automatic adjustment of the process, it will finally eliminate random manual readjustments and overcome current inkjet printing bottlenecks.

ACKNOWLEDGMENTS

This work has been partly supported by the Austrian Competence Centres for Excellent Technologies (COMET) programme (Grant No. 869301), operated by the Austrian Research Promotion Agency (FFG) on behalf of the Federal Ministry for Transport, Innovation and Technology (BMVIT) and the Federal Ministry for Digital and Economic Affairs (BMDW). Additional funding has also been provided by Land Steiermark and the Styrian Business Development Agency (SFG).

---

[1] H. A. Stone and L. G. Leal, Relaxation and breakup of an initially extended drop in an otherwise quiescent fluid, J. Fluid Mech. **198**, 399 (1989).

[2] A. A. Castrejón-Pita, J. R. Castrejón-Pita, and I. M. Hutchings, Breakup of Liquid Filaments, Phys. Rev. Lett. **108**, 074506 (2012).

[3] E. Lorenceau and D. Quéré, Drops impacting a sieve, J. Colloid Interface Sci. **263**, 244 (2003).

[4] H. Peng, N. Wang, D. Wang, and X. Ling, Experimental study on the critical characteristics of liquid atomization by a spinning disk, Ind. Eng. Chem. Res. **55**, 6175 (2016).

[5] C. Clanet and J. C. Lasheras, Transition from dripping to jetting, J. Fluid Mech. **383**, 307 (1999).

[6] J. A. Nicholls and A. A. Ranger, Aerodynamic shattering of liquid drops, AIAA J. **7**, 285 (1969).

[7] R. T. Collins, J. J. Jones, M. T. Harris, and O. A. Basaran, Electrohydrodynamic tip streaming and emission of charged drops from liquid cones, Nat. Phys. **4**, 149 (2007).

[8] A. L. Yarin, I. V. Roisman, and C. Tropea, *Collision Phenomena in Liquids and Solids* (Cambridge University Press, Cambridge, 2017).

[9] O. A. Basaran, Small-scale free surface flows with breakup: Drop formation and emerging applications, AIChE J. **48**, 1842 (2002).

[10] H. Sirringhaus, T. Kawase, R. H. Friend, T. Shimoda, M. Inbasekaran, W. Wu, and E. P. Woo, High-resolution inkjet printing of all-polymer transistor circuits, Science **290**, 2123 (2000).

[11] J. A. Rogers, T. Someya, and Y. Huang, Materials and mechanics for stretchable electronics, Science **327**, 1603 (2010).

[12] F. G. Zaugg and P. Wagner, Drop-on-demand printing of protein biochip arrays, MRS Bull. **28**, 837 (2003).

[13] C. Planchette, H. Pichler, M. Wimmer-Teubenbacher, M. Gruber, H. Gruber-Woelfler, S. Mohr, C. Tetyczka, W.-K. Hsiao, A. Paudel, E. Roblegg, and J. Khinast, Printing medicines as orodispersible dosage forms: Effect of substrate on the printed micro-structure, Int. J. Pharm. **509**, 518 (2016).

[14] J. F. Dijksman, Hydrodynamics of small tubular pumps, J. Fluid Mech. **139**, 173 (1984).

[15] T. W. Shield, D. B. Bogy, and F. E. Talke, Drop formation by dod ink-jet nozzles: A comparison of experiment and numerical simulation, IBM J. Res. Dev. **31**, 96 (1987).

[16] A.-S. Yang and W.-M. B. Tsai, Ejection process simulation for a piezoelectric microdroplet generator, J. Fluids Eng. **128**, 1144 (2006).
[17] Q. Xu and O. A. Basaran, Computational analysis of drop-on-demand drop formation, Phys. Fluids **19**, 102111 (2007).
[18] B. Derby, Inkjet printing of functional and structural materials: Fluid property requirements, feature stability, and resolution, Annu. Rev. Mater. Res. **40**, 395 (2010).
[19] H. Dong, W. W. Carr, and J. F. Morris, An experimental study of drop-on-demand drop formation, Phys. Fluids **18**, 072102 (2006).
[20] A. van der Bos, M.-J. van der Meulen, T. Driessen, M. van den Berg, H. Reinten, H. Wijshoff, M. Versluis, and D. Lohse, Velocity Profile Inside Piezoacoustic Inkjet Droplets in Flight: Comparison between Experiment and Numerical Simulation, Phys. Rev. Appl. **1**, 014004 (2014).
[21] J. Eggers and E. Villermaux, Physics of liquid jets, Rep. Prog. Phys. **71**, 036601 (2008).
[22] R. Collins, M. Harris, and O. Basaran, Breakup of electrified jets, J. Fluid Mech. **588**, 75 (2007).
[23] R. M. S. M. Schulkes, The contraction of liquid filaments, J. Fluid Mech. **309**, 277 (1996).
[24] P. Notz and O. Basaran, Dynamics and breakup of a contracting liquid filament, J. Fluid Mech. **512**, 223 (2004).
[25] T. Driessen, R. Jeurissen, H. Wijshoff, F. Toschi, and D. Lohse, Stability of viscous long liquid filaments, Phys. Fluids **25**, 062109 (2013).
[26] C. R. Anthony, P. M. Kamat, M. T. Harris, and O. A. Basaran, Dynamics of contracting filaments, Phys. Rev. Fluids **4**, 093601 (2019).
[27] S. D. Hoath, S. Jung, and I. M. Hutchings, A simple criterion for filament break-up in drop-on-demand inkjet printing, Phys. Fluids **25**, 021701 (2013).
[28] J. Hoepffner and G. Paré, Recoil of a liquid filament: Escape from pinch-off through creation of a vortex ring, J. Fluid Mech. **734**, 183 (2013).
[29] H. Dong, W. W. Carr, and J. F. Morris, Visualization of drop-on-demand inkjet: Drop formation and deposition, Rev. Sci. Instrum. **77**, 085101 (2006).
[30] J. B. Keller, Breaking of liquid films and threads, Phys. Fluids **26**, 3451 (1983).
[31] G. Sünderhauf, H. Raszillier, and F. Durst, The retraction of the edge of a planar liquid sheet, Phys. Fluids **14**, 198 (2002).